

# Compensated ionization chamber for (n, $\alpha$ ) reaction measurements at a spallation neutron source

Józef Andrzejewski,  
Yuri M. Gledenov,  
Andrzej Korejwo,  
Kamil Sobczak,  
Paweł J. Szałański

**Abstract.** The new spallation neutron facility n\_TOF (neutron time-of-flight) at CERN opens wide possibilities in measurements of neutron induced reaction cross sections. The facility with its excellent energy resolution of neutrons, low repetition rate and most important – with a very high instantaneous luminosity, makes up an extra challenge for experimenters faced by doing measurements at a high peak intensity spallation source. Our proposition is directed to the use of a compensated ionization chamber for the (n, alpha) reaction cross section measurements we plan to carry out in a wide range of neutron energy. First experience gained with using such a kind of detector at ORELA (the Oak Ridge Electron Linear Accelerator) neutron source (ORNL) was very optimistic.

**Key words:** ionization chamber • pulsed neutron source

## Peculiarity of measurements

Spectroscopic studies of charge particles such as the products of nuclear reactions induced by neutrons are carried out for many years [1, 2, 4, 14, 16]. In these measurements different detectors as well as many methods of detection are used to obtain nuclear data in the widest range of neutron energy. The best way to achieve this goal is to perform the experiment at pulsed neutron beams with the time-of-flight method for neutron spectrometry. The neutron beam energy distribution, however, is usually broad (white neutron source) and the flux in the narrow energy intervals is low, often some orders of magnitude smaller in comparison with the beams of charged particles accelerated in the machines like cyclotrons [10]. To achieve acceptable count rates of alpha particles from (n,  $\alpha$ ) reactions which are characterized by small cross section at low energy of neutrons, one ought: (i) to use possibly the biggest number of nuclei in target; (ii) to increase the efficiency of a detector by inserting it together with a target in a neutron beam (in such a way one can achieve almost 100% geometric efficiency in  $2\pi$  solid angle); (iii) to carry out a measurement during a long time.

In the case of alpha-particle spectroscopy, the target should be suitably thin (of the order of some hundreds of  $\mu\text{g}/\text{cm}^2$ ), what, in connection with condition (i), requires using the targets area from several tens to several thousands of  $\text{cm}^2$ . This is why semiconductor detectors were used in a few cases only [13, 18], while

J. Andrzejewski✉, A. Korejwo, K. Sobczak,  
P. J. Szałański  
Chair of Nuclear Physics and Radiation Safety,  
The University of Łódź,  
149/153 Pomorska Str., 90-236 Łódź, Poland,  
Tel.: +48 42 6355637, Fax: +48 42 6783958,  
E-mail: jozefan@uni.lodz.pl

Yu. M. Gledenov  
Joint Institute for Nuclear Research,  
Dubna, Russia

Received: 23 October 2006  
Accepted: 8 January 2007

in most cases gas detectors, such as ionization chambers or proportional counters, were used.

The merit of choice of gas detectors is: (a) opportunity to use a target with a large area and different form, (b) resistance of the detector to radiation damages, and at last (c) low cost of the detector. Additionally, in the case of ionization chamber with nuclear targets of large area, that is with large volume ( $V > 10 \text{ dm}^3$ ), there is no need to use the continuous flow and cleaning of a gas. Such detector keeps constant parameters even during three months of its work in the beam.

Presence of the overload effect of detector and amplifiers is an inherent feature of measurements of the  $(n, \alpha)$  reaction in the time-of-flight method. This effect is a result of the following factors:

1. Gamma flash generated in a neutron source based on slowing down electrons in a heavy target (bremsstrahlung effect).
2. Gamma flash and fast neutron stream emitted in pulsed nuclear reactors.
3. Gamma flash, fast neutron stream, muons and charged particles emitted in a spallation source.

Duration of the overload pulse limits the neutron energy unambiguously above which one is not able to measure reaction cross section and/or carry out spectrometry of alpha particles. Increasing the distance between the detector and neutron source and/or inserting into the beam a material filtering photons and fast particles can essentially shorten the duration of the pulse.

In consequence, in the first case the neutron flux is decreased, and thus the reaction count rate decreases according to  $1/r^2$  law. In the second case, however, it causes producing of 'holes' in some intervals of neutron energy additionally, corresponding to the position of neutron resonances for nuclides constituting the filters. The quantity of a construction material of the detector in beam path also plays a crucial role in the process of the "flash" pulse origin. The electrical charge produced in the detector by interaction of the particles with entrance and exit windows of the detector can be limited by inserting thin windows. If it is not possible with regard to the necessity of using gas under high pressure in the detector, thus the charge can be eliminated using screening electrodes with a potential equal to the potential of the closer electrode.

However, obtaining spectroscopic information in the neutron energy interval from several hundreds eV to 1 MeV – important for astrophysics – requires a solution different from that currently used.

### The aim of study

The main goal of study are  $(n, \alpha)$  reactions, which we are planning to perform for many nuclides in a wide range of target nuclei masses, and this may be an essential improvement in the determination of rates for reactions involving alpha particles inside stars. These values for reactions occurring in  $p$  process by which low abundance, proton-rich stable isotopes of intermediate to heavy elements were synthesized, belong to those calculated with the largest uncertainties. The knowledge about the details of  $p$  process is scarce; it seems that

the process takes place in the high temperature environment of massive stars or in supernovae [3]. Reactions involving  $\alpha$  particles, such as  $(\gamma, \alpha)$  or  $(\alpha, p)$ , play a very important role at such environment, but their rates are extremely difficult, or even impossible to determine in experiment. On the other hand, their theoretical calculations are hampered by large uncertainties achieving a factor of ten. As a result, the abundance of isotopes is estimated with similar uncertainty. The problem is connected mainly with uncertainties in the determination of the  $\alpha + \text{nucleus}$  optical potential in the astrophysically relevant energy range. Extrapolation of this potential value, obtained in a study of elastic scattering of alpha particles, has limited usefulness, because scattering measurements are carried out for energy higher than 12 MeV, that is beyond the astrophysically relevant energy range.

To better define the  $\alpha + \text{nucleus}$  optical potential, our group plans to carry out a series of  $(n, \alpha)$  reaction experiments in a wide range of masses and energies of nuclei. For resonance neutrons, the  $Q$ -values for  $(n, \alpha)$  reactions are such that the relative energy between the  $\alpha$  particle and residual nucleus are in the astrophysically interesting range, so no extrapolation is necessary. To match different optical potential in a statistical model of nuclear reactions and to compare calculated cross sections with obtained experimentally one can define the optimal potential. Its value permits to calculate with better accuracy reaction rates for the reactions involving alpha particles such as  $(\gamma, \alpha)$  and  $(\alpha, p)$ , important in  $p$ -process nucleosynthesis.

### Review of gas detectors used in the $(n, \alpha)$ reaction experiments at pulsed neutron source

In the study of alpha spectroscopy of the  $^{147}\text{Sm}(n, \alpha)$  reaction, initiated at Dubna at pulsed neutron sources (as an example in the considered problem), a double ionization chamber with a Frish grid was used, as shown in Fig. 1.

The chamber was adapted to mounting two back-to-back placed targets with a total area of about  $2500 \text{ cm}^2$  inside the working volume. To limit the overcharge of detector caused by fast neutrons and gammas, the collimated neutron beam irradiating the

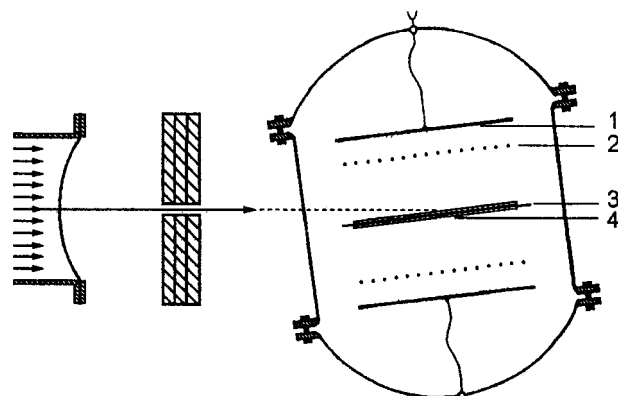


**Fig. 1.** Scheme of the double parallel plate ionization chamber. 1 – collector; 2 – grid; 3 – target backing; 4 – target [14].

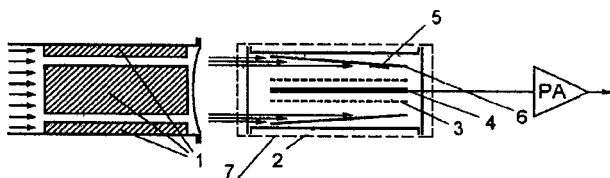


**Fig. 2.** Scheme of the cylindrical gridded ionization chamber located behind collimator of neutron beam. 1 – collimator; 2 – housing of the chamber; 3 – grid; 4 – collector; 5 – alpha source; 6 – target in the shape of truncated cone; 7 – Cd shield [16].

target at glancing angle of about  $4^\circ$  was used. Nevertheless, the neutron energy range was significantly limited due to the duration of the overload pulse: the upper limit was of  $E_n \approx 400$  eV for determining the (n,  $\alpha$ ) reaction cross section and of  $E_n \approx 240$  eV for obtaining alpha spectra for separate neutron resonances [16]. Later experiments were carried out with a new cylindrical gridded ionization chamber with a target shaped in the form of a lateral surface of truncated cone with an area of  $3700 \text{ cm}^2$  (Fig. 2). It gave the possibility to measure  $\sigma(n, \alpha)$  to the energy of  $E_n \approx 8.5$  keV and to register the pulse height spectrum of alpha particles for separate neutron resonances to the energy of 300 eV [2].

Such narrow interval of energy to a large extent results from limitation caused by a low energy resolution of neutron spectrometer equal to 48 ns/m in the considered study. In case of the  $^{143}\text{Nd}(n, \alpha)$  reaction, where the density of neutron resonances is low, the alpha particles spectra for separate resonances were obtained at energy up to  $E_n \approx 2600$  eV and  $\sigma(n, \alpha)$  up to  $E_n \approx 13$  keV under the same conditions as for  $^{147}\text{Sm}$  nuclei.

For performing the (n,  $\alpha$ ) reaction measurements at much higher energy of neutrons than mentioned previously, Koehler *et al.* [12] used a gas detector with the compensation method known for many years [19]. The prototype of the compensated ionization chamber designed for measurement of the  $^{17}\text{O}(n, \alpha)$  reaction was applied successfully [12].

The compensated ionization chamber (CIC), shown schematically in Fig. 3, consists of two ionization chambers with three flat-parallel electrodes. Outer electrodes are at an equal distance from the central signal electrode, and the voltages supplying them have opposite signs. The signals generated by the charge produced in both neighbouring chambers by a stream of gammas and particles penetrating them have opposite polarity. Both signals undergo compensation

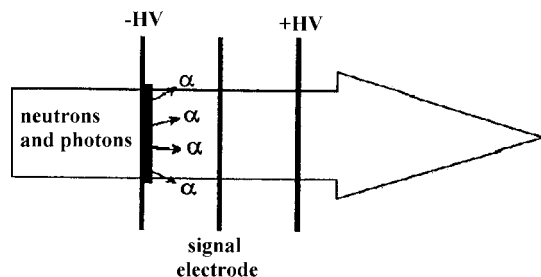


**Fig. 3.** A schematic view of one section of compensation ionization chamber.

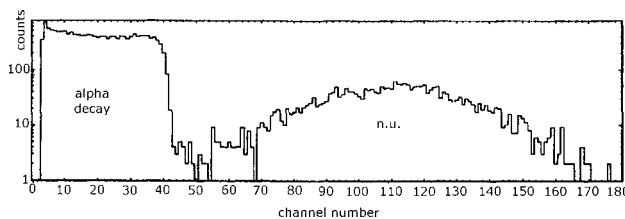


**Fig. 4.** Pulse-height spectrum from the  $^{147}\text{Sm}(n, \alpha)$  reaction and from alpha decay of  $^{147}\text{Sm}$ .

as a result of summing at the central electrode. Resultant signal should originate from the charge produced by a particle escaping the target only.

The first measurements of the  $^{147}\text{Sm}(n, \alpha)$  and  $^{143}\text{Nd}(n, \alpha)$  cross section in a wide neutron energy interval were carried out with an ORELA neutron spectrometer in Oak Ridge thanks to the adaptation of the existing ionization chamber as the compensated one [8, 11]. Although the CIC is characterized by a poorer pulse-height resolution (see Fig. 4) than, for example, a gridded ionization chamber, it reduces gamma flash effects by several orders of magnitude. It allowed measurements to be made up to 500 keV. In the experiment carried out at ORELA neutron beam the source-to-sample distance was 8.835 m and the neutron beam was collimated to 10 cm in diameter at the same position. Two samples were placed back-to-back in the centre of the parallel-plate CIC with the planes of the samples perpendicular to the neutron beam. Hence, the cross section was measured over nearly the entire  $4\pi$  solid angle. The sample was in the form of  $\text{Sm}_2\text{O}_3$  enriched to 95.3% in  $^{147}\text{Sm}$  and it had  $5.0 \text{ mg/cm}^2$  thickness by 11 cm in diameter.

The solution with using the compensated ionization chamber in the study of the  $^{37}\text{Ar}(n, \alpha)$  and  $^{39}\text{Ar}(n, \alpha)$  reactions with a neutron spectrometer GELINA was also realised by G. Goeminne *et al.* [9] in Geel. The measurements done by the CIC filled with  $\text{CH}_4$  resulted in data of the  $^{37}\text{Ar}(n, \alpha)^{34}\text{S}$  reaction cross section in the neutron energies range from 1 eV up to 10 keV.

#### Four-part compensated ionization chamber (FCIC)

Using the experience gained in Oak Ridge, an improved version of the compensated ionization chamber has been built at the University of Łódź. New detector has a cylindrical stainless steel housing of 2.0 mm thickness what allows to fill it with gas at a maximal pressure of 6 atm, several times higher than previously. Thanks to the increased working pressure, it is possible to put in the housing of a  $11.5 \text{ dm}^3$  volume four compensated ionization chambers (and four targets) under the condition that the distance between electrodes is longer than the maximal range of alpha particles. This ensures to carry out spectroscopic measurements, but with worse result than with the ionization chamber with Frish grid. The SHV connectors used in FCIC allow the electrodes to be supplied with voltages higher than in CIC. In particular, higher voltage allows the use of “faster” gases, with which an even better suppression of the  $\gamma$ -flash background can be attained. As a material of

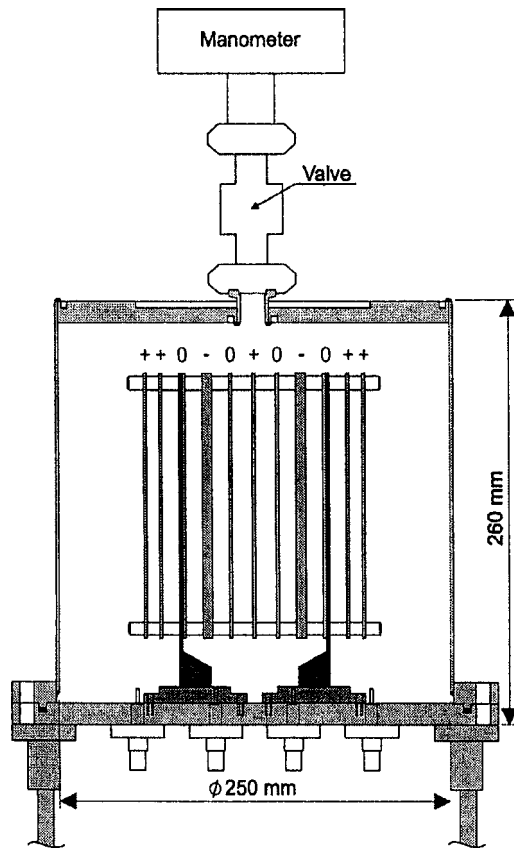


**Fig. 5.** Scheme of the four-part compensated ionization chamber.

electrodes, high purity aluminium was used with the aim to reduce the background generated by alpha particles from (n,  $\alpha$ ) reaction on lithium and boron contaminants characterized by a very high cross section. All insulators were made of Teflon and shaped in a way to prolong the path of a charge on the surface. Scheme of FCIC is shown in Fig. 5.

The detector has 11 high-purity Al foils as electrodes with dimension of  $14 \times 14$  cm mounted in aluminium frames making up four compensated chambers together. Signal electrodes through preamplifiers are at the same ground potential. Two outer electrodes are designed for screening the electrical charge generated by neutrons, photons and charge particles stream interacting with housing walls. High voltage supplies electrodes by a low-pass filter of  $RC = 4.4 \times 10^{-2}$  s. Electrodes are mounted on four horizontal Teflon rods and placed at an equal distance of 16 mm by means of distanced nuts. Tightness of the housing was checked by filling it with an argon gas and controlling the pressure during 2 weeks, taking into consideration the change of air temperature inside the room.

### Electron drift velocity in gas a mixture

Electron drift velocity is a basic parameter characterising operation speed of a gas detector. Initially FCIC was filled with Ar + 5% CO<sub>2</sub> gas mixture although it is known that CH<sub>4</sub> admixture allows to reach much higher drift velocity of electrons [5]. But interaction of neutron

beam with gas molecules, which include hydrogen atoms, increases the background generated by recoil protons. However, recoil nuclei produced by the interaction of fast neutrons with heavier atoms make sufficiently weaker background signals. So, the choice of CO<sub>2</sub> as admixture to argon results in lower background, but decreases by about 30% drift velocity of electrons. In the Ar + CO<sub>2</sub> gas mixture collecting time of electrons was determined with the use of an oscilloscope to measure the rise time of pulses after preamplifier for  $E/p$  value equal to 0.4 and 0.3 V/(cm·Torr). At the gas pressure  $p = 6$  atm, the collecting time  $t$  was 0.44 and 0.37  $\mu$ s, accordingly. These time values were recognised as too long and we decided to use a faster gas mixture, namely Ar + CF<sub>4</sub>.

We carried out measurement of electron drift velocity  $V_d$  for two mixtures of Ar + CF<sub>4</sub> by means of a simple set-up shown in Fig. 6, to compare the values with those presented in a few papers [6, 17, 20]. The method was based on determination of the drift time of electrons generated in ionization process by alpha particles emitted from <sup>235</sup>U. The knowledge of drift time and the distance covered by electrons moving from the place of origin to the grid allows determining their average drift velocity  $V_d$  in homogeneous electrical field.

Drift velocity was determined as a function of  $E/p$ , where  $E$  means the intensity of electrical field in the volume between cathode and grid, and  $p$  is the gas pressure in the chamber. The last value was constant and the  $E/p$  ratio was changing with change in the voltage that supplied electrodes. Collimator in vertical position with two gaps located at a distance of 7 mm from each other was used. The gaps were located in a way that the particle trajectories were parallel to the electrode planes and their upper edge was at the lower level of the edge of electrodes. Such solution insignificantly disturbed homogeneity of the electrical field just over the edge of the collimator.

Start of the generated pulse on the cathode is determined by the moment of appearance of electrons along the trace, and start of the pulse on the anode indicates the moment of crossing the electrons over the grid after drifting the way between the gap and the grid. Fast (electron) component of the pulse on the cathode rises to the moment when all drifting electrons cross the grid over and turn up in volume with electrical field  $E_2$ . Knowledge of the time between these pulses allows

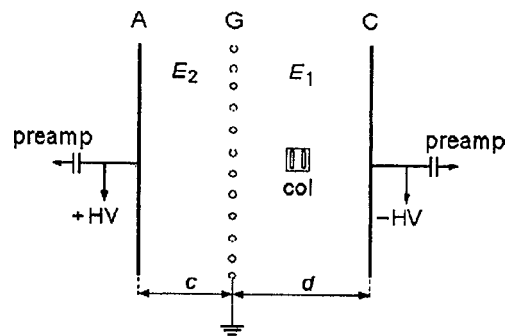


**Fig. 6.** Top view of the ionization chamber with grid used in the measurement of electron drift velocity (col – alpha source with collimator).

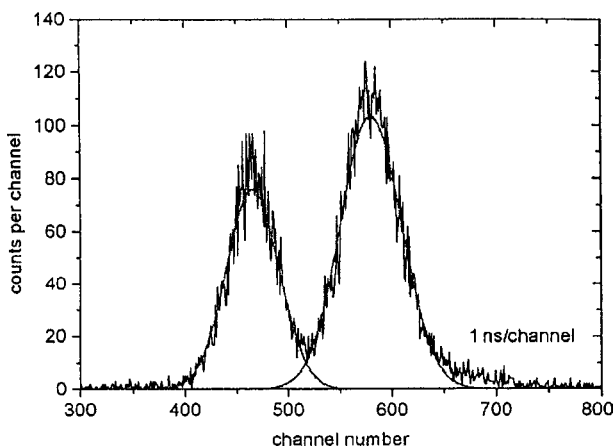


**Fig. 7.** An exemplary spectrum from TAC. Peaks correspond with the time-of-flight of electrons created along the centre of two gaps.

to determine the drift time of electrons  $t$ , and, at the same time, to calculate drift velocity. The time-amplitude converter TAC Ortec 547 was used to measure this time interval and the signals from TAC were sent to a multi-channel analyser. The use of collimator with two gaps causes that electron tracks appear at two different distances from the grid and in the obtained spectrum two peaks are seen, in accordance with two values of drift time. Knowing the distance between the gaps and the time difference corresponding to the position of two peaks, the drift velocity of electrons in the measured gas mixture was calculated.

An exemplary spectrum from TAC is shown in Fig. 7. Difference in heights of the peaks can be explained as the absence of homogeneity in thickness of the used  $^{235}\text{U}$  alpha source.

To increase accuracy of the calculated drift velocity of electrons, a correction factor was introduced taking into consideration the influence of the discrimination level on drift time. The calculation of drift time was performed by extrapolation of time distances (measured at a few discrimination levels) to zero value of discrimination level. Our results for the Ar +  $\text{CF}_4$  mixture are shown in Fig. 8.

In testing measurements, the chamber was filled with a mixture of 95% Ar + 5%  $\text{CF}_4$  for which the electron drift velocity at  $E/p = 0.4$  is 9.4 cm/ $\mu\text{s}$  (collecting time was 0.17  $\mu\text{s}$ ). This value is more than twice bigger than the value in the analogues mixture of Ar +  $\text{CO}_2$  at the same  $E/p$  [15] and is consistent with data published in paper [6].

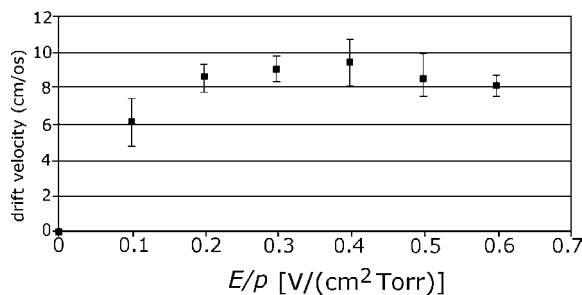


**Fig. 8.** Electron drift velocity for a mixture of Ar (95%) +  $\text{CF}_4$  (5%).

## Testing measurements

FCIC was checked tentatively with alpha particles from natural decay of uranium and  $^{147}\text{Sm}$  and then prepared to testing measurements on a pulsed neutron beam of n\_TOF facility at CERN [5]. This unique in the world neutron spectrometer produces neutron pulses by spallation reaction induced by pulsed 20 GeV proton beam on a massive Pb target block.

For test experiment, the housing was filled with a gas mixture of 95% Ar and 5%  $\text{CF}_4$  to a pressure of 6 atm. A sample (rectangle 9 cm by 13 cm, 5.0 mg/ $\text{cm}^2$  thick) of  $\text{Sm}_2\text{O}_3$  enriched to 95.3% in  $^{147}\text{Sm}$  was placed in one section. A second sample of  $^6\text{LiF}$  (11 cm in diameter, thickness of 80  $\mu\text{g}/\text{cm}^2$ ), to measure the reference  $^6\text{Li}(n, \alpha)^3\text{H}$  reaction, was placed in the second section. Signals from the collectors were amplified using Ortec 142 IH preamplifiers followed by active filter amplifiers (shaping time was 0.5  $\mu\text{s}$ ). The chamber was located downstream of PPAC and FIC1 (two detectors located in the beam) at a distance of 187 m from the neutron target block. The collectors were at ground potential and the sample electrodes were biased to  $-3000$  V. The FCIC electrodes was oriented perpendicular to the neutron beam direction with both the collectors upstream and downstream of the sample electrodes (at first and second run accordingly).

Output pulses from the amplifiers corresponding to the arrival of each pulse from the neutron production target at the FCIC were observed. As shown in Figs. 9 and 10, each pulse from the n\_TOF target induced an overload pulse in each FCIC. With no compensation voltage applied to the FCIC, these overload pulses always had the same shape; a positive lobe followed by a negative lobe, and afterwards by weakening oscillations lasting about 200  $\mu\text{s}$ . The positive polarity peak disappeared after applying a voltage of +500 V to compensating part of the chamber, but the negative pulse and oscillations remained (see Fig. 11). The amplitude of the negative lobe remained the same even though the negative high voltage was decreased to zero, and in fact remained unless the preamplifier was disconnected from the FCIC and had a Faraday cage put on its input. When the neutron beam was on, pulses from alpha

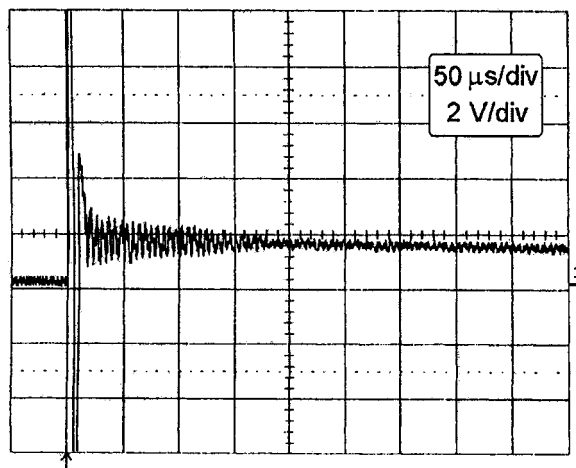


**Fig. 9.** Output pulses after amplifier without compensation (full range).

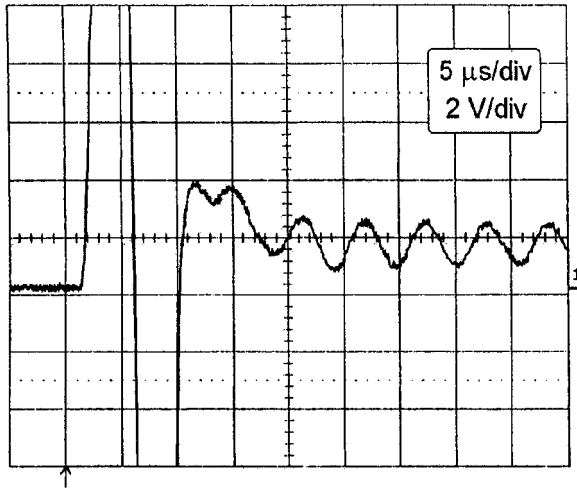


Fig. 10. Output pulses after amplifier (range selected).

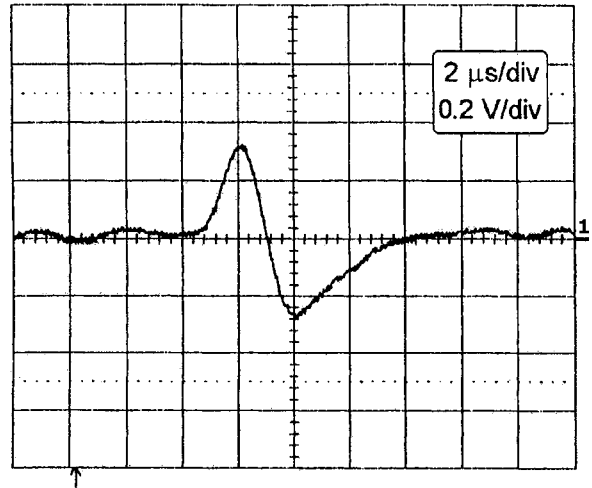


Fig. 13. Output pulses. The chamber was put away  $\sim 0.5$  m (out of the beam).

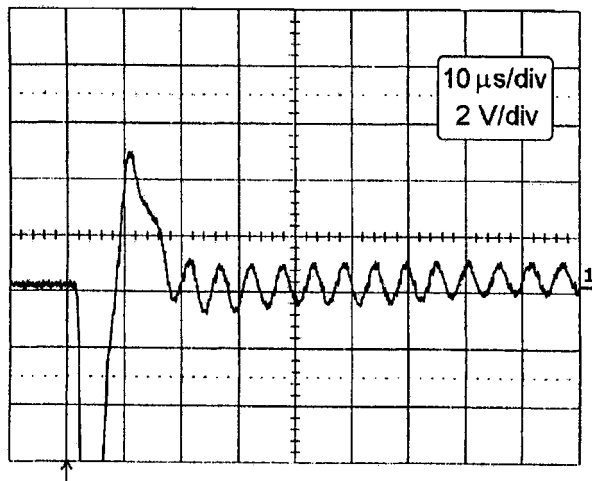


Fig. 11. Output pulses after amplifier (compensation switched on). The negative lobe and oscillations remained.

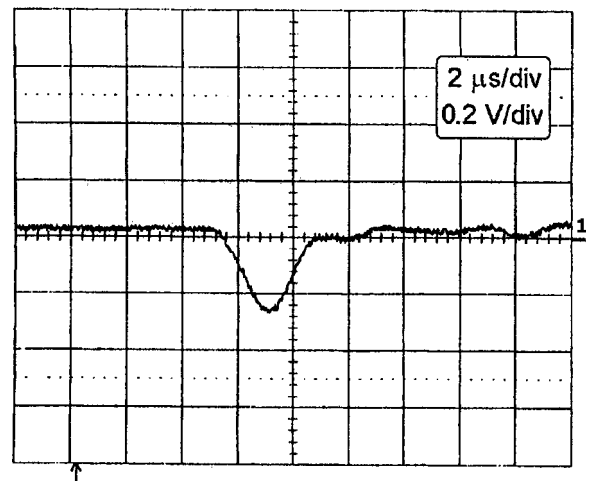


Fig. 14. Output pulses. The chamber was put away  $\sim 0.5$  m (out of the beam) with compensation voltage switched on.

decay of  $^{147}\text{Sm}$  were registered. One of them is shown in Fig. 12. The amplitude of these pulses remained the same for applied voltages between  $-500$  V to  $-3000$  V.

After moving the FCIC down  $0.5$  m so that it was out of the neutron beam, overload signals with similar

structure but lower amplitudes were observed, as shown in Fig. 13. The positive polarity lobe disappeared after applying a compensation voltage of  $+300$  V (see Fig. 14).

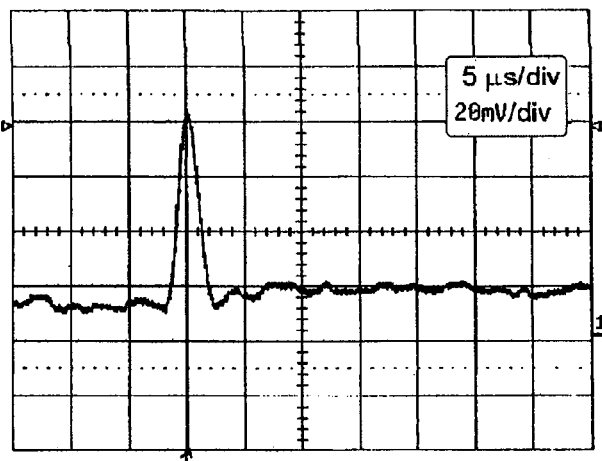


Fig. 12. Output pulse for alpha decay of  $^{147}\text{Sm}$ .

## Conclusions

On the basis of the results of test experiment we conclude that:

1. Compensation works well for cancelling the positive polarity lobe of the overload pulses. In a simple parallel-plate ionization chamber without grid, overload pulses are expected to have positive polarity because they are due to the gas ionization between the negatively polarized high voltage plate and the signal plate. Hence, the electrons from these events, drifting toward the collector induce a positive polarity pulse from the amplifier (the preamplifier is of the inverting type). In a FCIC, this signal is cancelled by another one of approximately equal magnitude arising from electrons drifting away from the collector towards the positive high voltage plate. The

positive overload pulse has the same polarity as the pulses corresponding to alpha particles from decay of  $^{147}\text{Sm}$  (or from  $^{147}\text{Sm}(n, \alpha)$  reactions).

2. The negative polarity lobe of the overload pulse probably is generated by ions knocked out from the collector and target material by fast charged particles and/or neutrons, that reach the FCIC after the gamma flash (which causes the positive lobe of the overload pulse). These two signals are not fully compensated because of short range of heavy ions at gas and followed the difference in distance of their tracks to the collector. The polarity of the summed signal is negative. The ions fly away from the collector inducing a positive polarity pulse on the collector (this pulse is inverted to negative polarity by the pre-amplifier) higher than the negative pulse from the target electrode. Its shape as well as the presence of this signal with no applied high voltage lead to this explanation.
3. The negative polarity lobe of the overload pulse is not due to electrical noise because it disappeared after disconnecting the preamplifier.
4. The persistence of an overload pulse (but with reduced amplitude and duration) even after the FCIC is removed from the beam indicates that the shielding and/or magnets used in n\_TOF allow some background particles and photons to leak through. Our conclusion is coherent with that presented in paper [7].

## References

1. Andrzejewski J, Vertebny VP, Vo Kim Tkhan, Vtyurin VA, Kiriluk AL, Popov YuP (1988) Study of (n,  $\alpha$ ) partial cross sections on  $^{143}\text{Nd}$ ,  $^{147}\text{Sm}$ ,  $^{149}\text{Sm}$  by filtered neutron beams. *Yadernaya Fizika (J Nucl Phys)* 48:20–25
2. Andrzejewski J, Vo Kim Tkhan, Vtyurin VA, Korejwo A, Popov YuP, Stępiński M (1980) Investigation of averaged cross sections for (n,  $\alpha$ ) reactions on  $^{123}\text{Te}$ ,  $^{143}\text{Nd}$ ,  $^{147}\text{Sm}$  and  $^{149}\text{Sm}$ . *Sov J Nucl Phys* 32:774–779
3. Arnould M, Takahashi K (1999) Nuclear astrophysics. *Rep Prog Phys* 62:395–464
4. Budtz-Jorgensen C, Knitter H-H (1984) A precise method for charged particle counting employing energy and angle information from gridded ion chambers. *Nucl Instrum Methods* 223:295–302
5. Cennini P, Abbondanno U, Alvarez H *et al.* (2002) n\_TOF facility, installation, performances. CERN n\_TOF facility: performance report. CERN/INTC-O-011, INTC-2002-037. CERN, Switzerland
6. Colas P, Delbart A, Derre J *et al.* (2002) Electron drift velocity measurements at high electric fields. *Nucl Instrum Methods Phys Res A* 478:215–219
7. Ferrari C, Rubbia C, Vlachoudis V (2002) A comprehensive study of the n\_TOF background at CERN. CERN SL-2002-011 (ECT). CERN, Switzerland
8. Gledenov YuM, Koehler PE, Andrzejewski J, Guber KH, Rauscher T (2000)  $^{147}\text{Sm}(n, \alpha)$  cross section measurements from 3 eV to 500 keV: implications for explosive nucleosynthesis reaction rates. *Phys Rev Rapid Comm C* 62:042801–042805
9. Goeminne G, Wagemans C, Wagemans J, Serot O, Loiselet M, Gaelens M (2000) Investigation of the  $^{37}\text{Ar}(n, p)^{37}\text{Cl}$  and  $^{37}\text{Ar}(n, \alpha)^{34}\text{S}$  reactions in the neutron energy range from 10 meV to 100 keV. *Nucl Phys A* 678:11–23
10. Koehler PE (2001) Comparison of white neutron sources for nuclear astrophysics experiments using very small samples. *Nucl Instrum Methods Phys Res A* 460:352–361
11. Koehler PE, Gledenov YuM, Andrzejewski J, Guber KH, Raman S, Rauscher T (2001) Improving explosive nucleosynthesis models via (n,  $\alpha$ ) measurements. *Nucl Phys A* 688:86–89
12. Koehler PE, Harvey JA, Hill NW (1995) Two detectors for (n, p) and (n,  $\alpha$ ) measurements at white neutron sources. *Nucl Instrum Methods Phys Res A* 361:270–276
13. Kvittek J, Hnatowicz V, Cervena J, Vacik J, Gledenov YuM (1981) Proton transitions in  $^{22}\text{Na}(n, p)^{22}\text{Ne}$  reaction. *Z Phys A* 299:177–178
14. Kvittek J, Popov YuP (1970) Investigation of the (n,  $\alpha$ ) reaction on Sm and Nd isotopes in the neutron energy region below 1 keV. *Nucl Phys A* 154:177–190
15. Peisert A, Sauli F (1984) Drift and diffusion of electrons in gases: a compilation, 84-08. CERN, Geneva
16. Popov YuP, Przytuła M, Rumi RF *et al.* (1972) Investigation of  $\alpha$ -decay of  $^{148}\text{Sm}$  resonance states. *Nucl Phys A* 188:212–224
17. Va'vra J, Coyle P, Kadyk J, Wise J (1993) Measurement of electron drift parameters for helium and  $\text{CF}_4$ -based gases. *Nucl Instrum Methods Phys Res A* 324:113–126
18. Wagemans J, Wagemans C, Goeminne G, Geltenbort P (2000) Experimental determination of the  $^{14}\text{N}(n, p)^{14}\text{C}$  reaction cross section for thermal neutrons. *Phys Rev C* 61:064601–064606
19. Wilkinson DH (1950) Ionization chambers and counters. Cambridge University Press, Cambridge
20. Yamashita T, Kobayashi H, Konaka A *et al.* (1989) Measurements of the electron drift velocity and positive – ion mobility for gases containing  $\text{CF}_4$ . *Nucl Instrum Methods Phys Res A* 283:709–715